2007 Urban Remote Sensing Joint Event

Damage mapping for the 2004 Niigata-ken Chuetsu earthquake using Radarsat images

Masashi Matsuoka
Earthquake Disaster Mitigation Research Center, NIED
Kobe, Japan
matsuoka@edm.bosai.go.jp

Fumio Yamazaki
Dept. Urban Environment Systems
Faculty of Eng., Chiba University
Chiba, Japan
yamazaki@tu.chiba-u.ac.jp

Hiroshi Ohkura
National Res. Inst. for Earth Science and Disaster Prevention (NIED)
Tsukuba, Japan
ohkura@bosai.go.jp

***Abstract*—The building damage detection technique which we have developed has been successfully applied to past events such as the earthquakes in Kobe in 1995, India in 2001, and Bam in 2003 by using the compound index, z-value, a value derived from the correlation and difference in intensities between pre- and post-event SAR images. This technique was applied to the areas affected in the Niigata-ken Chuetsu, Japan earthquake of October 23, 2004 by using one pair of Radarsat images taken before and after the earthquake. However, it was not possible to identify any significant distribution of damaged buildings. In this study, we examined the reasons for that and proposed a new technique that uses two pairs (pre-seismic and co-seismic) of SAR images to identify smaller building damage ratios in less densely built-up areas as compared to previous techniques. The main idea is to minimize the effects of signal noise and temporal changes of the earth's surface on building damage estimation by calculating the difference values of the two pre-event images and one post-event image. From a macroscopic point of view, the distributions of both difference values of the z-values and the correlation coefficients in built-up areas were in good agreement with damage reported in survey reports. In Yamakoshi village, located in the highlands, we could also identify large-scale landslides with accuracy as good as that of interpretation from aerial photos.**

I. INTRODUCTION

Recently, international frameworks have been formed to exploit the observation data of satellites launched by various countries, and remote sensing technology has been increasingly used as a means of early detection of the extent of the disasters that are occurring frequently across the globe. One such framework is the International Charter "Space and Major Disaster" [1], which aims to promote the contribution of earth observation satellites to disaster management. Based on this charter, an international cooperation mechanism which centers on space agencies has been established. Under this mechanism, areas where a disaster has occurred or is expected to occur are observed with an earth observation satellite on a priority basis, and the collected data is provided for free to the appropriate disaster prevention agencies to be utilized for emergency support, restoration, and for dealing with the aftermath.

Since 2003, the charter has been activated about 20 times a year, which indicates that large-scale natural disasters are occurring at the frequency of about twice a month globally. The thematic maps are published on the website1. As an example, areas damaged by the 2004 Sumatra-Andaman earthquake/tsunami could be roughly estimated with just 30 m spatial resolution, and with 1 m resolution, damage to buildings and bridges could be grasped visually [2,3]. However, since these visual interpretations are based on optical sensor images, damaged areas may not be visible due to clouds and cloud shadows, even if there is an early opportunity for observation. Satellites loaded with a synthetic aperture radar (SAR) are capable of observing the ground surface condition of a disaster-stricken area through clouds by day or night, but visual damage interpretation from SAR images is difficult, except in situations that have significant influences on backscattering properties, such as inundation due to flood. The International Charter "Space and Major Disaster" has published a few SAR-based thematic maps of damage to buildings, roads, and other social infrastructure. To use SAR images for damage detection, appropriate image processing is essential.

We, the authors, have previously proposed a technique to automatically detect areas of large-scale damage, such as collapsed buildings [4], based on the comparison of backscattering intensity recorded on SAR images (two scenes) taken from the satellite which observed the disaster-stricken area before and after the 1995 Kobe earthquake. We have confirmed the validity of our technique through its application to other earthquake damage [5,6]. In this paper, we apply the SAR damage detection technique to the 2004 Niigata-ken Chuetsu earthquake in order to ascertain the practical limits of the technique by means of comparison with the building damage survey data in Ojiya city. We also propose a new technique which is applicable to less densely built-up areas and capable of detecting damage in moderately affected areas through an additional pre-earthquake SAR data.

II. APPLICATION OF PREVIOUS DAMAGE DETECTION METHOD

A. Outline of Damage Detection Method

Since the Kobe earthquake in 1995, comparative studies between building damage and intensity or phase information of SAR images have been actively performed [5,7,8]. What is especially important is that the intensity information obtained from SAR does not largely depend on observation conditions such as orbit. Therefore, a change detection technique based on intensity information is highly portable to other areas.

Below, we will explain the outline of our idea/technique for damaged area detection, as deduced from field survey data and SAR images observed by ERS satellites of the European Space Agency before and after the Kobe earthquake [4,5].

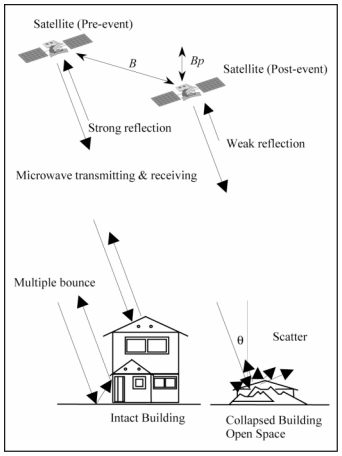

Figure 1. Schematic figure of observation with the satellite SAR.

Backscattering intensity is affected by wavelength and incidence angle of the microwave, as well as dielectric properties and the irregularity of the ground surface. When we focus on the irregularity of the ground surface alone, the microwave irradiated from the satellite to the urban area and the backscattering intensity increases due to plural reflections between the ground surface and the buildings (cardinal effect) as shown in Fig. 1. On the other hand, in the case of a microwave sent to open areas and areas of collapsed buildings, the components that return to the satellite are small due to multidirectional scattering. This change can be expressed by the correlation coefficient and the difference of the backscattering coefficient σ^0 (dB) before and after the earthquake.

After the accurate registering of SAR images of two periods, we apply a speckle reduction filter [9] with a 21 × 21 pixel window to each image. We calculate the difference values, *d*, for the average of the backscattering coefficient in the 13 × 13 pixel window (equation (1)) and the correlation coefficient, *r*, from the 13 × 13 pixel window (equation (2)). Then, we detect the damaged area based on the compound variable (discriminant score, *z*) that employs the difference and the correlation coefficient as explanatory variables as shown in equation (3).

$$d = 10 \cdot \log_{10} \bar{Ia}_i - 10 \cdot \log_{10} \bar{Ib}_i \tag{1}$$

$$r = \frac{N\sum_{i=1}^{N} Ia_i Ib_i - \sum_{i=1}^{N} Ia_i \sum_{i=1}^{N} Ib_i}{\sqrt{\left(N\sum_{i=1}^{N} Ia_i^{\,2} - \left(\sum_{i=1}^{N} Ia_i\right)^2\right)\cdot\left(N\sum_{i=1}^{N} Ib_i^{\,2} - \left(\sum_{i=1}^{N} Ib_i\right)^2\right)}} \tag{2}$$

$$z = -2.140\, d - 12.465\, r + 4.183 \tag{3}$$

where *i* is the sample number, and if the images are of two period, i.e., before and after the event, Ia_i and Ib_i are the digital numbers of the post- and pre-images, respectively. $\bar{Ia}_i$ and $\bar{Ib}_i$ are the corresponding averaged digital numbers over the surroundings of pixel *i* within a 13 × 13 pixel window; the total number of pixels *N* within this window is 169, which is used to compute the two indices. A pixel with a high *z* value is assigned as a severely damaged area. Focusing on detection of building damage within urbanized areas, the pixels with backscattering coefficients smaller than the assigned threshold value of approximately –5 dB to –6 dB are masked in the *z* value distribution. The filter and window sizes used were empirically determined to reduce speckle noise and increase the accuracy of damage interpretation based on comparisons between ERS (Earth Resources Satellite) images of pixel size 30 m and building damage survey data [10], sorted by city blocks following the Kobe earthquake.

B. Application to the 2004 Niigata-ken Chuetsu Earthquake

On October 23, 2004, an earthquake of magnitude (Mw) 6.5 occurred in the Chuetsu area, Niigata Prefecture, and caused serious damage: 40 people died, approx. 3, 000 people were injured, and more than 10,000 residential houses collapsed completely or partially. The earthquake also caused significant damage to road facilities, agricultural facilities, and lifelines due to slope failures, liquefactions, etc. Particularly, in the former Yamakoshi village, located close to the epicenter, where the frequency of landslide occurrences is one of the highest in Japan, many slope failures and landslides occurred. Since the earthquake occurred in the evening, damage information collected immediately after the earthquake was limited.

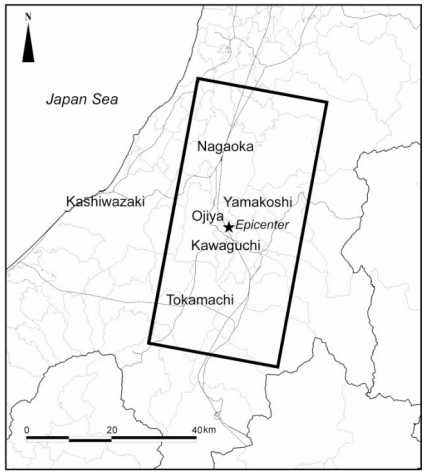

Figure 2. Scope of analysis of the 2004 Niigata-ken Chuetsu earthquake (rectangular portion).

Two days after the earthquake, the Canadian Space Agency's SAR-loaded Radarsat satellite observed the disaster-stricken area in fine mode (C band, HH polarization, approx. 9m spatial resolution). For our study, we performed a geometric correction and conversion on backscattering intensity from SLC (Single Look Complex) data. Fig. 2 shows the area of the image. There is a pre-earthquake observational

image from October 1, 2004. We applied the technique described above to Radarsat images taken before and after the earthquake and examined the detection of building damage areas. Fig. 3 shows the result of zoom-in image around Ojiya city which is one of the most severe damaged cities. Unlike the Kobe earthquake [4] or the 1991 Kocaeli earthquake in Turkey [5], almost no damage is detected in the affected area.

In the following sections, based on data compiled from the building damage survey conducted after the earthquake in Ojiya city, we will evaluate the results of the detection and proceed with the development of a technique that can detect the building damage in Ojiya city.

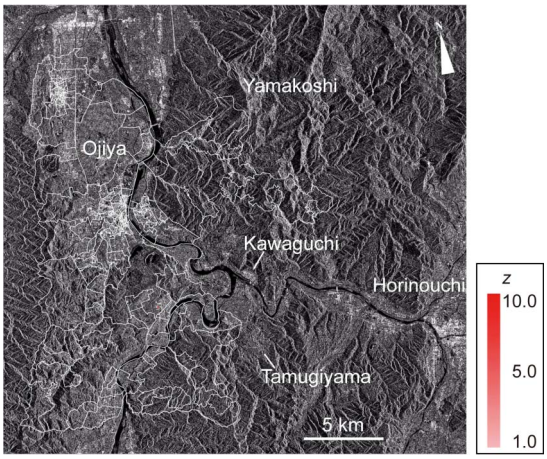

Figure 3. Zoom-in distribution of discriminant score z around Ojiya city extracted from Radarsat/Fine images. (The background represents the intensity image observed on October 1, 2004. The white line represents the administrative border of Ojiya city.)

III. Relationship between Building Damage and Backscattered Property

A. *Damage in Ojiya City*

In Ojiya city, located relatively close to the epicenter, the result of building damage survey was compiled as a GIS database [11]. According to the survey data, about 3,300 residential houses were completely or partially collapsed. While the severe damage rate of buildings including non-residential houses aggregated by the unit of machi (town) and aza (village section) was around 0% to 20% in the city center, it was 10% to 50% in the northeast, west, and southwest parts of the city, higher than in the city center [11]. The building density, however, differs significantly depending on the area.

To identify the areas of severe damage more clearly and examine the reason why the estimated damage distribution based on the technique described in Fig. 3 failed to explain the actual damage situation, comparing damage and building density with that of the 1995 Kobe earthquake (which served as the basis for the development of the detection technique). As explained above, since this detection technique is based on the cardinal effect of building groups peculiar to SAR images and its change, building density and the expansiveness of urban areas are important factors.

According to the GIS data of the Kobe earthquake [10], the average building density in the urban areas is one building per approx. 580 m^2; the building density in the Kobe area is relatively high. This means that there are about 100 houses per 250 m cell (area is 62,500 m^2). When we divided the area into 250 m cells, we took into consideration the fact that the road portion outside the city block would be included, and that floor plans are generally more spacious in provincial cities than in large cities. When we selected the areas with more than 50 buildings in a 250 m cell as built-up areas in Ojiya city and compared with damage distribution in the Kobe area, high building density is limited to an extremely narrow area in Ojiya city, which predominantly shows a severe-damaged building rate of less than 12.5%.

Therefore, if we combine this examination with the precedent reports [4,5,6], it is apparent that this damage detection technique is estimated to be applicable in high-densely built-up urban areas with complete building

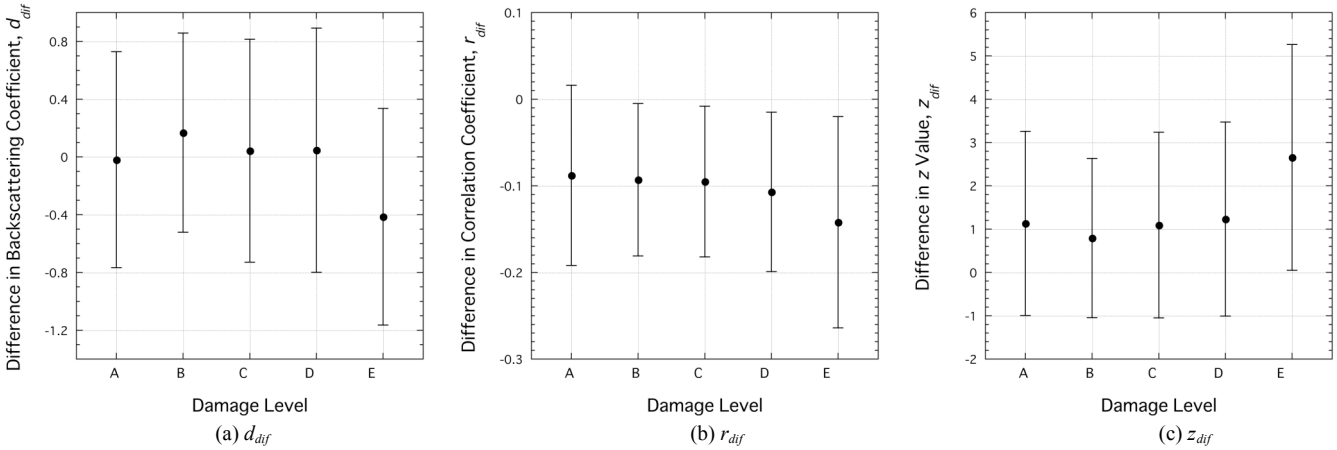

Figure 4. Relationship between the change of backscattered property and building damage level of Ojiya city. (A: severe damage rates 0 to 6.25%, B: 6.25 to 12.5%, C: 12.5 to 25%, D: 25 to 50%, E: 50 to 75%).

collapse rates of 25% or above.

B. Relationship between Differences of Backscattered Properties and Severe Damage Rates

As we explained in the preceding subsection, it has become clear that this damage detection technique, which is mainly based on the phenomenon of decreasing cardinal effect after an earthquake, has limited application, despite its simplicity of using only two scenes taken before and after the earthquake. Accordingly, we attempted to develop a new damage detection technique that is applicable to areas that contain small-scale municipalities, accepting a greater number of scenes.

Since there is an observational image of the Chuetsu-area in Niigata Prefecture on September 7, 2004, taken earlier than the Radarsat image (October 1st, 2004), we added it as a pre-event image for this study. From the pre-event image pair, we calculated differences of the backscattering coefficient (d_{bb}), correlation coefficient (r_{bb}), and discriminant score (z_{bb}) using the equations (1) - (3). Then, we obtained the difference of backscattering coefficients differences ($d_{dif} = d - d_{bb}$), the difference of correlation coefficients ($r_{dif} = r - r_{bb}$), and the difference of discriminant scores ($z_{dif} = z - z_{bb}$) from the d, r and z already calculated from the pair of pre-event and post-event images, in order to examine the relationship between the changes of these indices and the severe-damaged building rates.

For this examination, it is necessary to sample areas in which buildings existed beforehand. In the detection technique explained in Sec. II, we selected areas of large backscattering intensity in the pre-event image, assuming the cardinal effect of the building groups. In this study, we selected areas of small variations (with stable backscattering property) in the pre-event image pair in order to take advantage of the newly added pre-event image. We employed coherence [12] for the data set of this study, because the baseline length Bp of the pre-event images was rather short, about 340 m. Coherence is more sensitive to the irregularity of the ground surface and is suitable for distinguishing building groups [12]. We calculated the coherence from a 5 × 5 pixel window and established a threshold of 0.3 from its spatial distribution. We sampled the areas with values larger than the threshold as the subject of study, assuming that they are highly probable to have buildings.

Fig. 4 shows the relationship between the damage level based on the 250 m grid cell data of the damage survey result of Ojiya city and the differences of various indices, d_{dif}, r_{dif} and z_{dif}. Areas where the number of subject buildings in the cell is less than ten and areas that include snow-induced damage after the SAR data acquisition are excluded. Here, the damage levels are classified into five categories based on the severe-damaged building rate. Considering precedent studies [5], the severe damage rates 0 to 6.25%, 6.25 to 12.5%, 12.5 to 25%, 25 to 50%, and 50 to 75% are defined to be damage level A, B, C, D, and E, respectively. As the number of pixels applicable in each damage level varies, we sampled 1,000 pixels from each level at random, then obtained the average value and standard deviation. From a macroscopic point of view, we can interpret from Fig. 4 that the d_{dif} and r_{dif} values decrease as the damage level goes up, and the z_{dif} value becomes larger accordingly. This is consistent with our assumption in Sec. II that backscattering intensity decreases and the correlation coefficient also reduces in the damaged area. According to the variance analysis, the F-ratio becomes significant at the significance level of 1% between the damage levels A and E. Correlation rates are $z_{dif} > d_{dif} > r_{dif}$ in descending order, and the difference of discriminant scores, z_{dif}, proves to be most suitable for classifying the damage levels. However, while the r_{dif} value increases or decreases in consistency with the trend of the damage level, the z_{dif} and d_{dif} values of the damage level B are inverted, and there are variations in trend within the small damage level.

IV. Detection of Damage Area Using Differences of Correlation Coefficients

As we described above, for the selection of areas to be studied (areas with stable backscattering property), we used coherence calculated from the phase information. However, this value is strongly dependent on observation conditions such as the baseline length, Bp, and observation interval [7], and there is little opportunity to utilize it. However, the correlation of intensity images is not extensively bound by image observation conditions [7]. Therefore, when we consider the practical acquisition of damage conditions at the time of the disaster or emergency, it is more feasible to use the correlation coefficient. Accordingly, we conceived an idea to use the correlation coefficient r_{bb} calculated from a pair of pre-event images for the selection of the subject area. Constant values for the correlation coefficient can be obtained even when the calibration of pixel values is insufficient. If damaged area detection is feasible only with the correlation coefficient, it becomes possible to develop a more redundant damage detection system.

Fig. 5 shows the distribution of the difference of correlation coefficients r_{dif} overlaid on the intensity image. The areas of which r_{bb} value is 0.8 or larger are defined as the subject areas. Areas that have a higher probability of damage are painted with warmer colors. The areas with small r_{dif} value are distributed from Ojiya city to Kawaguchi-machi, the areas which suffered severe damage. On the other hand, in Nagaoka city and Tokamachi city, the values are large. This is in good agreement with the report [13] that investigated the building damage over a wide area. The areas where the severe-damaged building rate is 50% or above almost correspond to the area where the r_{dif} value is –0.15 or below. In the figure, areas with small r_{dif} values (green and red) are present locally in the mountainous areas around former Yamakoshi village, and their distribution is in good agreement with the locations of slope failures [14] interpreted from aerial photographs and with the damaged area estimated from the vegetation index of the IKONOS satellite [15]. We consider the correlation coefficient to have been reduced as the irregularity of the ground surface changed due to landslides and slope failures. As to the mountainous areas, however, due to the influences of lay over, foreshortening, and shadow effects peculiar to SAR images, there are cases that are difficult to detect depending on their locations.

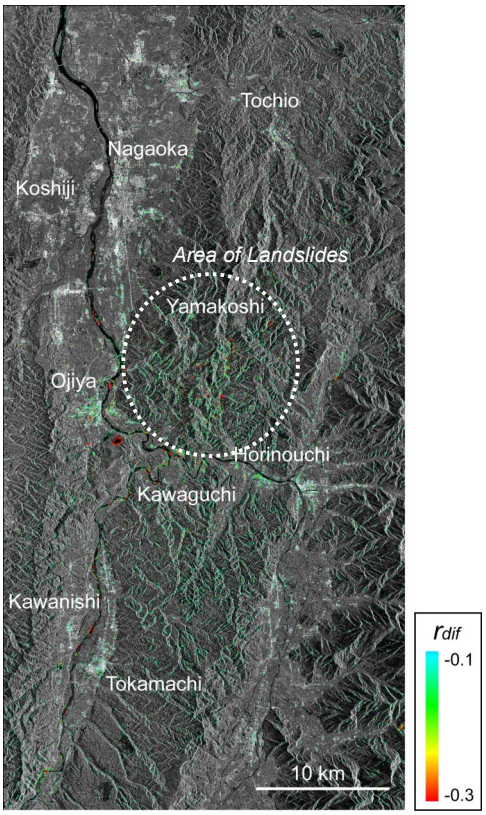

Figure 5. Distribution of the difference of correlation coefficients r_{dif} calculated from Radarsat/Fine image. (The background represents the pre-event intensity image taken on October 1, 2004.) The subject areas are where the correlation coefficient of the pre-event image pair is 0.8 or above.

In the case of damage detection solely dependent on the correlation coefficient, areas where water boundaries change significantly, such as river bars and regulating reservoirs, are also detected. To avoid these misinterpretations, it is essential to compare the detection result with the original image rather than reading the damaged area solely from the detection result based on image processing.

V. CONCLUSION

We applied the building damage area detection technique, which is based on the composite variable (discriminant score) calculated from the changes of the backscattering coefficient and correlation coefficient of pre- and post-event satellite SAR images (two scenes), to the Radarsat images of the 2004 Niigata-ken Chuetsu earthquake. We also used the building damage survey data from Ojiya city to determine the limitations of the technique in less densely built-up areas. Using three image scenes (with the addition of a new pre-event scene), we calculated the post-event variances of the correlation coefficient and discriminant score as compared to those in a stationary state (obtained from the pre-event pair of images) and studied their relationship to the severe-damaged building rates. As a result, it was proved that these differences and the damage levels closely correspond, and that damage can be detected even in less densely built-up areas. The technique that is solely dependent on the correlation coefficient also suggests the possibility of detecting areas of slope failures.

ACKNOWLEDGMENT

A part of this research was made possible by the grant-in-aid for scientific research (Research No. 17510155). Radarsat is owned by the Canadian Space Agency. We would like to extend our thanks to these supports.

REFERENCES

[1] International Charter "Space and Major Disaster," http://www.disasterscharter.org/, 1999.

[2] F. Yamazaki, M. Matsuoka, P. Warnitchai, S. Polngam, and S. Ghosh, "Tsunami reconnaissance survey in Thailand using satellite images and GPS", *Asian Journal of Geoinformatics, Asian Association on Remote Sensing*, Vol.5, No.2, 2005, pp.53-61.

[3] H. Miura, A. Wijeyewickrema, and S. Inoue, "Evaluation of tsunami damage in the eastern part of Sri Lanka due to the 2004 Sumatra earthquake using remote sensing technique", *8th U.S. National Conference on Earthquake Engineering*, Paper No.856, 2006.

[4] M. Matsuoka and F. Yamazaki, "Use of satellite SAR intensity imagery for detecting building areas damaged due to earthquakes", *Earthquake Spectra*, Vol.20, No.3, 2004, pp.975-994.

[5] M. Matsuoka and F. Yamazaki, "Detection of building damage areas due to earthquakes using satellite SAR intensity images", *Journal of Structural and Construction Engineering, Architectural Institute of Japan*, No.551, 2002, pp.53–60 (in Japanese with English abstract).

[6] M. Matsuoka and F. Yamazaki, "Building damage mapping of Iran earthquake using Envisat/ASAR intensity imagery", *Earthquake Spectra*, Vol.21, No.S1, 2005, pp.S285-S294.

[7] C. Yonezawa and S. Takeuchi, "Decorrelation of SAR data by urban damages caused by the 1995 Hyogoken-Nanbu earthquake", *International Journal of Remote Sensing*, Vol.22, No.8, 2001, pp.1585-1600.

[8] Y. Ito, M. Hosokawa, H. Lee, and J. G. Liu, "Extraction of damaged regions using SAR data and neural networks", *19th Congress of International Society for Photogrammetry and Remote Sensing (ISPRS2000)*, Vol.33, Part B1, 2002, pp.156-163.

[9] J. S. Lee, "Digital image enhancement and noise filtering by use of local statistics," *Transactions on Pattern Analysis and Machine Intelligence*, Vol.2, No.2, 1980, pp.165–168.

[10] Building Research Institute (BRI), *Final Report of Damage Survey of the 1995 Hyogoken-Nanbu Earthquake*, Building Research Institute, 1996 (in Japanese).

[11] K. Horie, H. Hayashi, N. Yoshitomi, K. Shigekawa, S. Tanaka, and N. Maki, "Applicability of Damage Assessment Total Support System using GIS through a response activity following 2004 Niigata-ken Chuetsu earthquake disaster", *2005 ANCER Annual Meeting*, CD-ROM, 2005.

[12] H. A. Zebker and J. Villasenor, "Decorrelation in interferometric radar echoes", *Transactions on Geoscience and Remote Sensing*, Vol.30, No.5, 1992, pp.950-959.

[13] M. Yoshimi, T. Komatsubara, Y. Miyachi, K. Kimura, K. Yoshida, H. Sekiguchi, M. Saeki, M. Ozaki, T. Nakazawa, R. Nakashima, S. Kunimatsu, and H. Saomoto, "Preliminary report on the 23 October 2004 Niigata-ken Chuetsu earthquake: Landforms and local site effects in heavily damaged areas", *Chishitsu News*, No.607, 2005, pp.18-28 (in Japanese).

[14] Geological Survey Institute, "Disaster map: distribution of landslide due to the 2004 Niigata-ken Chuetsu earthquake", http://zgate.gsi.go.jp/niigatajishin/ (in Japanese).

[15] H. Miura and S. Midorikawa, "Slope failure by the 2004 Niigata-ken Chuetsu, Japan earthquake observed in high-resolution satellite images", *4th International Workshop on Remote Sensing for Post-Disaster Response*, CD-ROM, 2006.